RESEARCH ARTICLE OPEN ACCESS

Diffusion Tensor Imaging in Boys With Adrenoleukodystrophy

Identification of Cerebral Disease and Association With Neurocognitive Outcomes

Elizabeth I. Pierpont, PhD,* René Labounek, PhD,* Ashish Gupta, MD, MPH, Troy Lund, MD, PhD, Paul J. Orchard, MD, William B. Dobyns, MD, Monica Bondy, BS, Amy Paulson, BS, Andrew Metz, MD, Ryan Shanley, MS, Jeffrey R. Wozniak, PhD, Bryon A. Mueller, PhD, Daniel Loes, MD, David Nascene, MD, and Igor Nestrasil, MD, PhD

Correspondence
Dr. Pierpont
pier0053@umn.edu

Neurology® 2024;103:e209764. doi:10.1212/WNL.0000000000209764

Abstract

Background and Objectives

Childhood cerebral adrenoleukodystrophy (C-ALD) is a severe inflammatory demyelinating disease that must be treated at an early stage to prevent permanent brain injury and neurocognitive decline. In standard clinical practice, C-ALD lesions are detected and characterized by a neuroradiologist reviewing anatomical MRI scans. We aimed to assess whether diffusion tensor imaging (DTI) is sensitive to the presence and severity of C-ALD lesions and to investigate associations with neurocognitive outcomes after hematopoietic cell therapy (HCT).

Methods

In this retrospective cohort study, we analyzed high-resolution anatomical MRI, DTI, and neurocognitive assessments from boys with C-ALD undergoing HCT at the University of Minnesota between 2011 and 2021. Longitudinal DTI data were compared with an age-matched group of boys with ALD and no lesion (NL-ALD). DTI metrics were obtained for atlas-based regions of interest (ROIs) within 3 subdivisions of the corpus callosum (CC), corticospinal tract (CST), and total white matter (WM). Between-group baseline and slope differences in fractional anisotropy (FA) and axial (AD), radial (RD), and mean (MD) diffusivities were compared using analysis of covariance accounting for age, MRI severity (Loes score), and lesion location.

Results

Among patients with NL-ALD (n = 14), stable or increasing FA, stable AD, and stable or decreasing RD and MD were generally observed during the 1-year study period across all ROIs. In comparison, patients with mild posterior lesions (Loes 1–2; n = 13) demonstrated lower baseline FA in the CC splenium (C-ALD 0.50 ± 0.08 vs NL-ALD 0.58 ± 0.04; $p_{BH} = 0.022$ adjusted Benjamini-Hochberg *p*-value), lower baseline AD across ROIs (e.g., C-ALD 1.34 ± 0.03 $\times 10^{-9}$ m^2/s in total WM vs NL-ALD 1.38 ± 0.04 $\times 10^{-9}$ m^2/s; $p_{BH} = 0.005$), lower baseline RD in CC body and CST, and lower baseline MD across ROIs except CC splenium. Longitudinal slopes in CC splenium showed high sensitivity and specificity in differentiating early C-ALD from NL-ALD. Among all patients with C-ALD (n = 38), baseline Loes scores and DTI metrics were associated with post-HCT neurocognitive functions, including processing speed (e.g., FA WM Spearman correlation coefficient R = 0.64) and visual-motor integration (e.g., FA WM R = 0.71).

Discussion

DTI was sensitive to lesion presence and severity as well as clinical neurocognitive effects of C-ALD. DTI metrics quantify C-ALD even at an early stage.

*These authors contributed equally to this work as co-first authors.

From the Departments of Pediatrics (E.I.P., R.L., A.G., T.L., P.J.O., W.B.D., M.B., A.P., I.N.), Neurology (A.M.), Psychiatry & Behavioral Sciences (J.R.W., B.A.M.), and Radiology (D.N.), University of Minnesota Medical School, Minneapolis; Biostatistical Design and Analysis Center (R.S.), Clinical and Translational Science Institute, University of Minnesota, Minneapolis; and Independent Neuroradiologist-Consultant (D.L.), Minneapolis, MN.

Go to Neurology.org/N for full disclosures. Funding information and disclosures deemed relevant by the authors, if any, are provided at the end of the article.

The Article Processing Charge was funded by the authors.

Glossary

AD = axial diffusivity; **ALD** = adrenoleukodystrophy; **ANCOVA** = analysis of covariance; **BH** = Benjamini-Hochberg; **C-ALD** = cerebral adrenoleukodystrophy; **CC** = corpus callosum; **CST** = corticospinal tract; **DTI** = diffusion tensor imaging; **FA** = fractional anisotropy; **FLAIR** = fluid-attenuated inversion recovery; **FSL** = FMRIB Software Library; **GRAPPA** = generalized autocalibrating partially parallel acquisition; **HCT** = hematopoietic cell-based therapy; **JHU** = John Hopkins University; **MD** = mean diffusivity; **MPRAGE** = magnetization-prepared rapid gradient echo; **NL-ALD** = adrenoleukodystrophy with no lesion; **RD** = radial diffusivity; **ROI** = region of interest; **TE** = echo time; **TI** = inversion time; **TR** = repetition time; **WM** = white matter.

Introduction

Adrenoleukodystrophy (ALD) is a rare X-linked disorder of peroxisomal function caused by pathogenic variants in the *ABCD1* gene that lead to the accumulation of very long chain fatty acids across organ systems, including the adrenal glands and nervous system.[1] The most severe expression of this disorder is cerebral adrenoleukodystrophy (C-ALD), a phenotype characterized by progressive inflammatory demyelinating brain lesions. Approximately 35%–40% of male patients with ALD develop C-ALD in childhood, with typical onset between 3 and 12 years.[2,3] Hematopoietic cell-based therapies (HCTs) with matched donor stem cells or autologous gene-corrected cells have demonstrated efficacy to halt the progression of C-ALD.[4-6] However, HCT must be performed at an early stage to preserve neurocognitive function.[7] The severity of cerebral lesions is conventionally assessed using the radiologic scoring system developed by Loes, which tallies the number and extent of brain structures affected by lesions on anatomical MRI.[8] The Loes score at the time of HCT predicts survival, disease progression, and risk of long-term neurocognitive and neuropsychiatric impairments.[9,10]

Over the past decade, the gradual expansion of newborn screening for ALD has enabled presymptomatic MRI surveillance of boys with *ABCD1* gene variants, thus facilitating earlier C-ALD detection and treatment.[11] A review of anatomical MRI by a clinical neuroradiologist is the standard method to detect and characterize lesions, but early radiologic changes are often subtle and challenging to identify.[12] Moreover, the anatomical MRI is unable to detect changes in white matter (WM) integrity in areas outside of the visible lesion. The emergence of new treatments for C-ALD has demonstrated a need for unbiased, objective metrics sensitive to subtle changes in WM microstructure that would support the early detection of C-ALD and the evaluation of therapeutic response in future clinical trials.

Diffusion tensor imaging (DTI) assesses WM integrity based on local properties of water molecule diffusion and has been proposed as a potential early disease marker for ALD.[13,14] Unlike the Loes score, DTI is sensitive to changes in normal-appearing WM and can quantify the degree of degradation within a specific region of interest (ROI).[15,16] These properties suggest that DTI may be useful for clinical monitoring and as a potential surrogate outcome measure in longitudinal ALD clinical trials.[13,17]

This observational study analyzed DTI acquired over a 1-year interval in 2 ALD patient groups. The first group consisted of boys with C-ALD who underwent HCT. The Loes score at the pre-HCT evaluation defined C-ALD disease severity. The second group included boys with ALD without cerebral lesions ("no lesion" group; NL-ALD) who were being monitored for potential development of C-ALD. Because demyelinating lesions are nearly always first observed in the corpus callosum (CC) or corticospinal tract (CST) projection fibers (i.e., within the brainstem, internal capsule),[2,18] we focused DTI analyses on these ROIs, comparing them with total WM. Four working hypotheses were evaluated. The first hypothesis asserts that DTI metrics in the CC and CST are sensitive to mild, early-stage C-ALD lesions. The second hypothesis asserts that DTI changes in boys with mild C-ALD are detectable in normal-appearing WM. The third hypothesis asserts that individuals with NL-ALD have stable WM maturation trajectories. The fourth hypothesis asserts that DTI metrics are associated with the development of neurocognitive symptoms in patients with C-ALD.

Methods

Participants

Our analysis included boys with ALD between 3 and 15 years of age evaluated at the University of Minnesota Medical Center over a 10.5-year period (May 1, 2011, to November 1, 2021). Figure 1 depicts patient selection. Of 66 individuals who underwent HCT for C-ALD, a subset of 38 boys had MRI scans with the same DTI acquisition protocol at 2 time points ~1 year apart: an initial scan at 1.4 ± 0.8 months before HCT and a follow-up scan 12.3 ± 1.1 months after HCT (interscan interval: 13.5 ± 1.3 months; range: 11.1–16.3 months). Treatment protocols involved preparative regimens, followed by either an allogeneic HCT or an autologous HCT using genetically modified stem cells. An age-matched comparison group of 14 untreated boys with ALD without cerebral lesions was identified among those undergoing routine MRI surveillance during this same period. Individuals were included in the NL-ALD group if they had MRI scans using

Figure 1 Study Selection

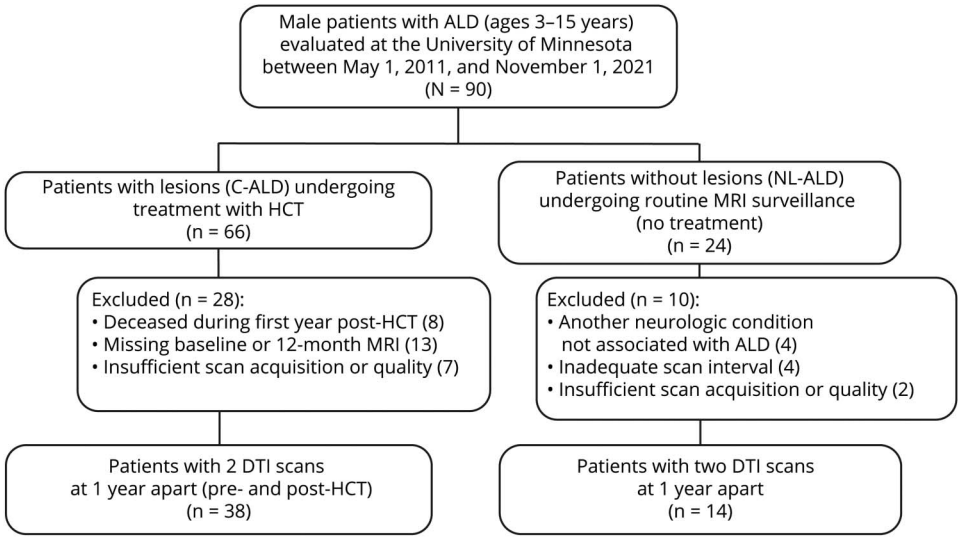

ALD = adrenoleukodystrophy; C-ALD = cerebral adrenoleukodystrophy; DTI = diffusion tensor imaging; HCT = hematopoietic cell-based therapy; NL-ALD = adrenoleukodystrophy with no lesion.

the same DTI acquisition protocol approximately 1 year apart (interscan interval: 13.3 ± 1.6 months; range: 11.3–17.0 months). All patients with NL-ALD had confirmed elevations in very long chain fatty acids and at least one of the following: (1) an *ABCD1* variant classified as pathogenic or likely pathogenic or (2) a family history of an ALD phenotype. The 14 boys in the NL-ALD group were followed for a median of 2.1 years (range: 1.0–8.1 years) past the second scan; 1 of the 14 has since developed C-ALD. Those with insufficient/missing DTI acquisition or with another neurologic condition not associated with ALD were excluded from both groups.

Standard Protocol Approvals, Registrations, and Patient Consents

Written informed consent was obtained from parents or guardians of all study participants enrolled in clinical research studies for observation or treatment of ALD. Retrospective MRI and neurocognitive data analysis was approved with waiver of informed consent by the University of Minnesota Institutional Review Board (STUDY00002247).

MRI

Brain MRI was performed on a 3T scanner (Siemens Skyra) with a 20-channel head/neck coil located at the University of Minnesota Masonic Children's Hospital. High-resolution anatomical images were acquired using sagittal 3-dimensional T1-weighted magnetization-prepared rapid gradient echo (MPRAGE) without a contrast agent (Figure 2). MPRAGE acquisition parameters included repetition time (TR) = 1,900 milliseconds, echo time (TE) = 2.19 milliseconds, inversion time (TI) = 900 milliseconds, voxel size 0.9 × 0.9 × 0.9 mm^3, flip angle 9°, and generalized autocalibrating partially parallel acquisition (GRAPPA) acceleration factor = 2. Axial 2-dimensional T2-weighted fluid-attenuated inversion recovery (FLAIR) with fat saturation and T2-weighted fat-suppressed turbo spin echo sequences were also collected as part of the MRI ALD surveillance protocol (Figure 2). FLAIR acquisition parameters were TR/TE/TI 9,000/81/2,500 milliseconds, voxel size 0.6 × 0.6 × 4.0 mm^3, flip angle 150°, and GRAPPA = 2. T2 acquisition parameters were TR/TE 4,000/79 milliseconds, voxel size 0.5 × 0.5 × 4.0 mm^3, flip angle 150°, and GRAPPA = 2. The DTI protocol was acquired to quantify cerebral tissue microstructural integrity (e.g., mean diffusivity (MD) and fractional anisotropy (FA) maps in Figure 2). Parameters of DTI were TR/TE 6,300/95 milliseconds, posterior-anterior phase-encoding direction, 12 unique bipolar gradient waveform directions with the multidirectional diffusion weighting mode, b = 1,000 s/mm^2 acquired twice without averaging, 2 b_0 scans, and voxel size 1.875 × 1.875 × 5.000 mm^3 (70 scans; 67% of the data set) or 2.188 × 2.188 × 5.000 mm^3 (34 scans; 33% of dataset). Because DTI metrics are dependent on voxel size,[19,20] voxel volume was used as a covariate in statistical comparisons.

Radiologic Scoring

Loes scores were ascertained on a scale of 0–34 (higher scores indicate more severe disease) by review of MPRAGE, T2, and FLAIR images by a board-certified neuroradiologist (D.L. or D.N.) who was blinded to the DTI metrics and neurocognitive status of the patients. Before analysis, patients were categorized into one of 7 subgroups for comparison and visualization of DTI results. Stratification of patients with C-ALD based on pre-HCT Loes score, and disease pattern was informed by recent studies demonstrating that both the severity and location of the lesion are relevant factors in predicting clinical outcomes.[7,9,21,22] Subgroups were as follows: no lesion (Loes 0; n = 14); mild posterior lesion (Loes 1–2; n = 13); mild/moderate lesion (Loes 2.5–4.5) in posterior (n = 5), frontal (n = 2), or atypical (n = 4) WM

Figure 2 Representative Examples of FLAIR and MPRAGE Scans With MD and FA Maps in 2 Similar-Aged Boys With ALD

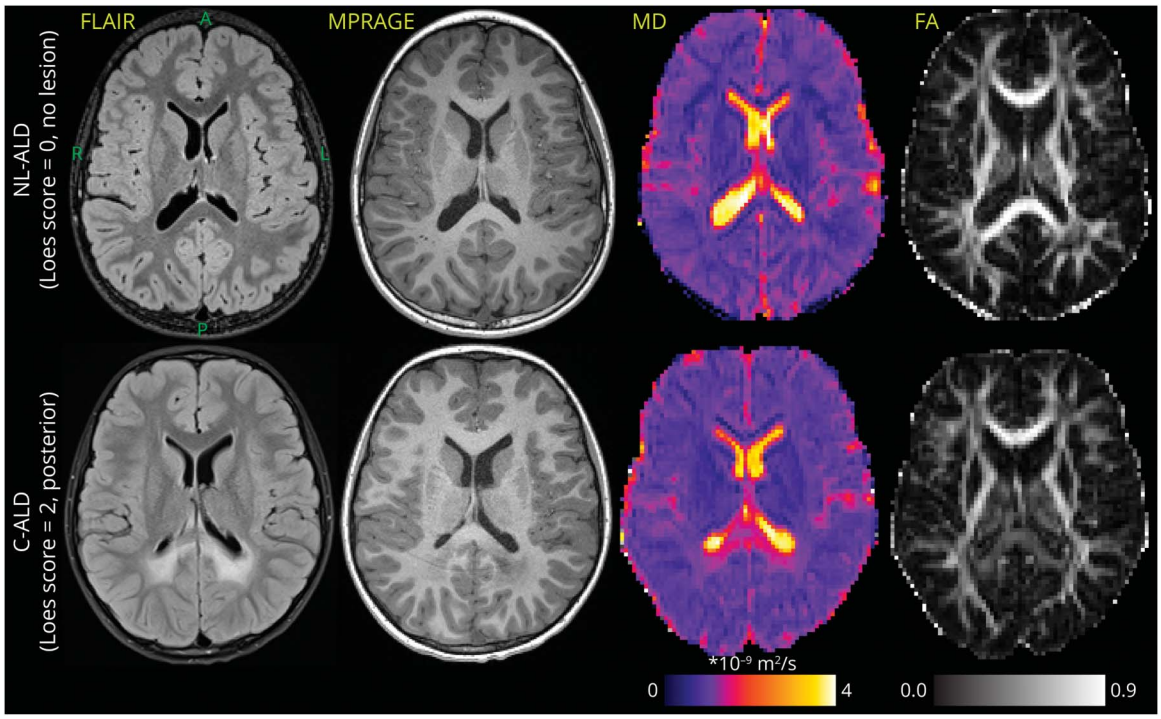

Top row: patient without cerebral demyelinating disease. Bottom row: patient with posterior pattern C-ALD affecting the CC splenium and adjacent parietal-occipital WM (Loes = 2). Axial slices follow the orientation noted for the left top image (A = anterior, P = posterior, R = right, L = left). The interpatient slice location was matched as closely as possible across different MRI contrasts. ALD = adrenoleukodystrophy; C-ALD = cerebral adrenoleukodystrophy; FA = fractional anisotropy; FLAIR = fluid-attenuated inversion recovery; MD = mean diffusivity; MPRAGE = magnetization-prepared rapid gradient echo; WM = white matter.

locations; moderate posterior lesion (Loes 5–8.5; n = 4); and severe posterior lesion (Loes 9+; n = 10). For all patients with posterior or frontal disease, lesions were observed to affect the CC (the splenium or genu, respectively), whereas atypical disease patterns affected portions of the CST (e.g., in the brainstem or internal capsule), anterior temporal WM, and/or auditory pathway without involvement of the CC.

Lesion Segmentation

To facilitate analysis of the sensitivity of DTI metrics to the disease process in normal-appearing WM, lesion segmentation was performed so that voxels within visible lesions could be identified. For C-ALD cases, lesions were outlined semi-automatically in the MPRAGE scans with ITK-SNAP visualization software (version 3.6) using an automated 3-dimensional image contour segmentation tool.[23] Output labels were then edited and manually corrected as necessary.

DTI Preprocessing and Analysis

Cerebral microstructure analysis was conducted with a fully automated pipeline. DTI data were analyzed with in-house implemented scripts using FMRIB Software Library (FSL, version 6.0.1).[24] Eddy current–induced distortions and motion artifacts were corrected with the eddy_correct function using spline interpolation. Brain masks were estimated using the bet function and averaged eddy corrected image.[25] Diffusion tensor was estimated in each brain voxel using the dtifit function. Fractional anisotropy (FA) maps were nonlinearly co-registered with the 1-mm FA template included in the John Hopkins University (JHU) WM atlas using the fsl_reg function and contrast set to the FA value; subsequently, the JHU WM atlas labels were warped into native space of the DTI scan.[26-31] For C-ALD scans, the FA map was also co-registered to the MPRAGE scan using affine image registration and mutual information as a similarity criterion using the flirt function.[29,30] The outlined lesion was warped into the native space of the DTI scan. The warped JHU WM atlas identified ROIs in the native diffusion space. The JHU-based ROIs included total WM (i.e., all non-zero voxels belonging to WM tracts in the atlas), CST, CC genu, body, and splenium. Averaged FA and mean (MD), radial (RD), and axial (AD) diffusivities were estimated for each ROI and scan using 2 approaches: (1) from all voxels of the ROI (fully automated approach) and (2) from only normal-appearing voxels in the ROI (semiautomated approach excluding voxels within the segmented lesion). Higher FA and lower MD values generally indicate better microstructural integrity.[32] Longitudinal trends in DTI metrics in ROIs were characterized as slopes, with the number of years between scans defining between-scan time intervals for slope estimation.

Neurocognitive Assessment

For patients with C-ALD, 6 neurocognitive domains were assessed during clinical neuropsychological evaluations at baseline and 1 year after HCT. Using methods established in previous longitudinal ALD studies reporting cognitive outcomes,[7,10] verbal reasoning, visual reasoning, working memory, and processing speed were evaluated using age-appropriate versions of the Wechsler scales. Fine motor dexterity was evaluated with the Purdue Pegboard test (average of dominant, nondominant, and both hand trials). Visual-motor integration was evaluated with the Beery-Buktenica Test of Visual-Motor Integration. Age-adjusted standard scores were used for all neurocognitive tests. Details regarding neurocognitive measurement methodology are described in the eMethods.

Statistical Analysis

Between-group differences in DTI metrics and longitudinal slopes were investigated with analysis of covariance (ANCOVA) using age and voxel volume as covariates. To account for multiple comparisons, adjusted Benjamini-Hochberg (BH) p-values were reported to reduce the false discovery rate ($p_{BH} < 0.05$). The adjusted p_{BH}-values were estimated from the complete set of original uncorrected p-values of all DTI metrics and ROIs separately for the baseline and slope tests. The original uncorrected p-values are provided in eTable 1 including descriptive statistics of baseline, follow-up, and slope measures. For boys with C-ALD, associations between baseline DTI metrics and 1-year post-HCT neurocognitive scores were assessed using Spearman correlation coefficients, with corresponding CIs calculated using Fisher transformation method. To further estimate the relationship between DTI and neurocognitive metrics while accounting for individual differences at baseline, a follow-up analysis evaluated associations between longitudinal changes in DTI metrics and neurocognitive functions (i.e., the difference between baseline and year 1) using Spearman correlation coefficients.

Data Availability

Bash and Matlab scripts used for analysis of DTI data and overall statistical analysis for this study are available at github.com/umn-milab/qmri-ald (release v1.0.1'). The scripts and deidentified DTI data set are available for the purposes of replicating procedures and results. With the exclusion of any patients enrolled in an ongoing and/or unpublished clinical trial, deidentified neurocognitive data are available from the corresponding author upon request.

Results

Characteristics of the study cohort are listed in Table 1. The C-ALD and NL-ALD groups were similar in age at baseline, with Loes scores ranging from 1 to 19 among patients with C-ALD. Thirteen patients with C-ALD demonstrated Loes scores between 1 and 2, constituting a subgroup of patients with "mild" lesions. All patients with mild lesions had a posterior disease pattern starting in the CC splenium, with or without involvement of parietal-occipital WM. This subgroup was, on average, younger (mean age: 6.3 ± 1.9 years) than the overall C-ALD cohort and the NL-ALD group; age was, therefore, included as a covariate in statistical comparisons.

Table 1 Study Cohort Characteristics

	C-ALD (n = 38)	NL-ALD (n = 14)
Age at initial scan, y, mean (SD); range	8.2 (2.8); 4.7–14.9	8.0 (3.7); 3.3–14.0
Age at follow-up scan, y, mean (SD); range	9.3 (2.8); 5.8–15.6	9.1 (3.8); 4.2–15.0
Radiologic severity, mean (SD); range		
Loes MRI score at initial scan	5.5 (4.7); 1–19	0
Loes MRI score at follow-up scan	8.3 (6.0); 1.5–23	0
Demyelination pattern, n		
Parietal-occipital variant	32/38	N/A
Frontal variant	2/38	N/A
Atypical variant (no callosal lesion)	4/38	N/A

Abbreviations: C-ALD = cerebral adrenoleukodystrophy; NL-ALD = adrenoleukodystrophy with no lesion.

Cross-Sectional Analysis

The sensitivity of DTI to the presence and severity of WM lesions was assessed with a cross-sectional comparison of ALD subgroups. Figure 3 shows baseline DTI metrics in the CC splenium for subgroups with posterior lesions. Among patients with more severe lesions (i.e., with higher Loes scores), FA values were generally lower and RD values higher. FA better distinguished patients without lesions from those with mild lesions. AD was lower in patients with mild lesions as compared with those without lesions but showed higher values among patients with more severe disease. The CC body, CC genu, CST, and WM ROIs showed similar findings (eFigures 1–4), although less pronounced than in the CC splenium.

To evaluate whether DTI metrics distinguished patients without demyelinating lesions from those with mild posterior C-ALD lesions (Loes: 1–2), metrics for the baseline scan were compared across these 2 groups (Table 2). The results of the ANCOVA demonstrated that the group with mild C-ALD showed lower FA and AD in the CC splenium compared with the NL-ALD group. In addition, AD was lower in CC, CST, and total WM ROIs for the mild C-ALD group at baseline. These results were similar for MD, except for the CC splenium. RD was lower in the CC body and CST. Similar results were obtained when voxels classified as lesion were excluded

Figure 3 Box Plots Depict Baseline DTI in the CC Splenium for Patients With a Posterior Disease Pattern

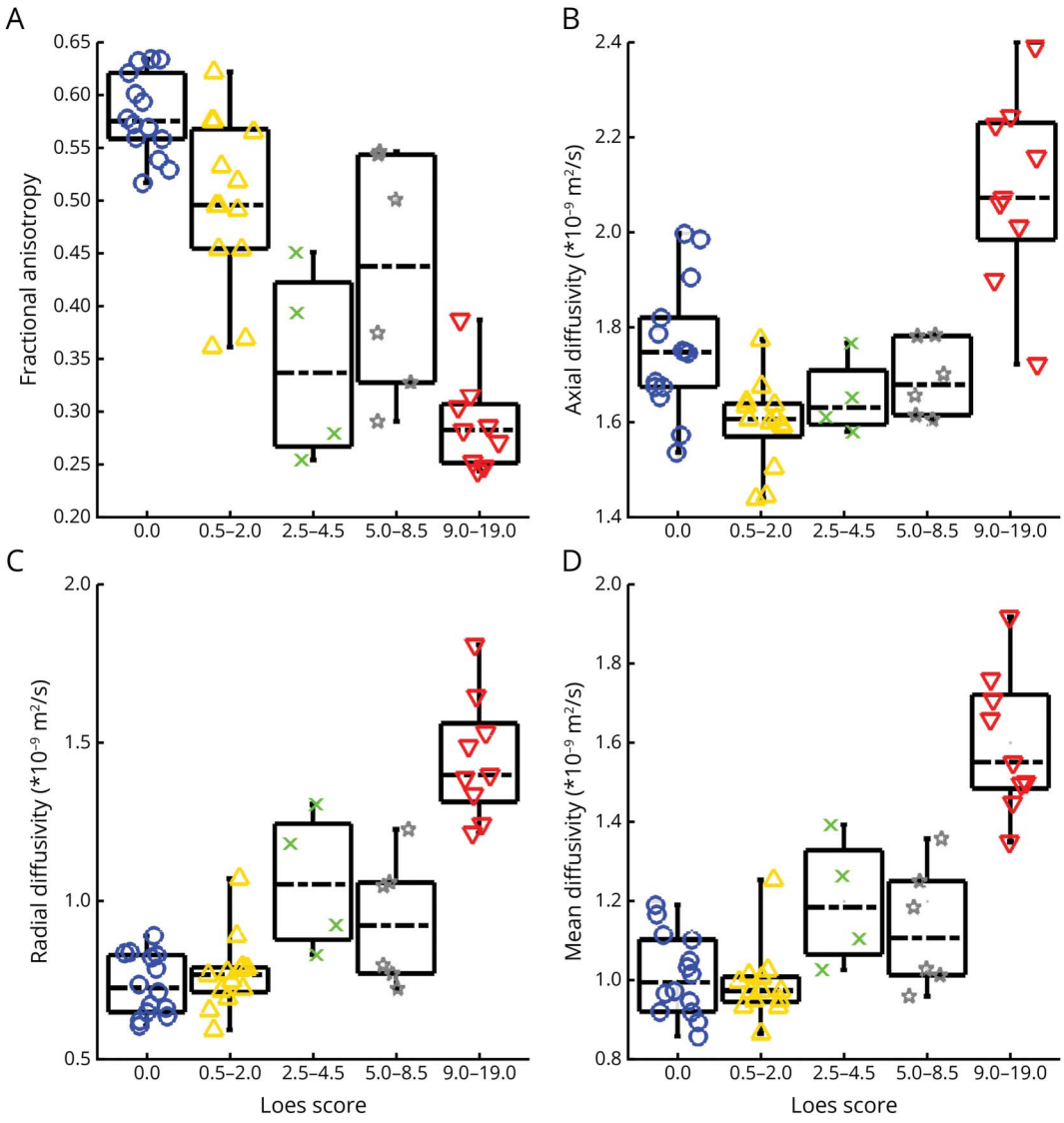

(A) Lower FA was associated with higher MRI severity (i.e., Loes score) in C-ALD patients. CC splenium FA was lower in patients with mild C-ALD lesions (0 < Loes ≤ 2; yellow triangles) compared with those without lesions (blue circles). (B) AD in the CC splenium was lower in patients with mild C-ALD (yellow triangles) relative to those without lesions (blue circles) but demonstrated higher values in those with more severe lesions (i.e., higher Loes score). (C and D) Radial and mean diffusivity were similar in patients with mild C-ALD relative to those without lesions; these metrics were higher with more severe lesions (i.e., with higher Loes score). Patients with lesions in frontal or corticospinal tracts were not included in this figure because of the small sample sizes. AD = axial diffusivity; ALD = adrenoleukodystrophy; C-ALD = cerebral adrenoleukodystrophy; CC = corpus callosum; DTI = diffusion tensor imaging; FA = fractional anisotropy.

from the ROI-based analysis (eTable 2). DTI was sensitive to early demyelinating C-ALD processes even in the portions of ROIs that appeared normal on standard anatomical MRI scans.

Figure 4A visualizes longitudinal DTI results for FA in the cerebral WM, subdivisions of the CC, and CST for each patient. Among boys in the NL-ALD group, FA generally increased, whereas RD and MD decreased across regions over time (see also Table 2), consistent with the typical pattern of WM development in healthy children.[33,34] Slope values (mean ± SD) were calculated for a time interval measured in years, that is, an expected per-year change. Positive slopes indicating increasing FA values (slope >0) were frequently observed in patients with NL-ALD, especially in the CC splenium (86%; slope = 0.011 ± 0.015 per year) and genu (93%; slope = 0.015 ± 0.021 per year). However, in boys with mild posterior C-ALD, FA in the CC typically declined in the 1-year period after HCT, with decreasing values in 92% of patients in the splenium (slope = −0.073 ± 0.102 per year) and 100% in the genu (slope = −0.016 ± 0.021). Figure 4B visualizes FA slope discriminability between patients with NL-ALD and mild C-ALD across all ROIs. Sensitivity and specificity values can be derived from Table 2.

Table 2 Comparison of Cross-Sectional and Longitudinal DTI Metrics in a Group of Patients With ALD Without Lesions (No Lesion; n = 14) and a Group With Mild Posterior C-ALD Lesions (Mild Lesion; n = 13) Across 5 Regions of Interest

	No lesion Loes = 0		Mild lesion 0 < Loes ≤ 2		ANCOVA p_{BH} values		Frequency of slope >0, n (%)	
ROI	Baseline	Follow-up	Baseline	Follow-up	Baseline comparison	Slope comparison	No lesion (total n = 14)	Mild lesion (total n = 13)
Fractional anisotropy								
WM	0.45 ± 0.03	0.46 ± 0.03	0.45 ± 0.02	0.43 ± 0.02	0.7811	**0.0028**	12 (86)	3 (23)
CC splenium	0.58 ± 0.04	0.59 ± 0.04	0.50 ± 0.08	0.42 ± 0.09	**0.0221**	**0.0347**	**12 (86)**	**1 (8)**
CC genu	0.56 ± 0.04	0.57 ± 0.04	0.56 ± 0.03	0.54 ± 0.03	0.5662	**0.0028**	**13 (93)**	**0 (0)**
CC body	0.48 ± 0.05	0.49 ± 0.05	0.49 ± 0.05	0.46 ± 0.05	0.4834	**0.0030**	10 (71)	3 (23)
CST	0.57 ± 0.04	0.59 ± 0.04	0.57 ± 0.03	0.56 ± 0.03	0.3356	**0.0042**	13 (93)	4 (31)
Axial diffusivity								
WM	1.38 ± 0.04	1.39 ± 0.06	1.34 ± 0.03	1.34 ± 0.05	**0.0052**	0.5669	9 (64)	8 (62)
CC splenium	1.76 ± 0.14	1.76 ± 0.12	1.60 ± 0.09	1.73 ± 0.20	**0.0043**	0.1136	6 (43)	10 (77)
CC genu	1.59 ± 0.06	1.60 ± 0.08	1.52 ± 0.04	1.55 ± 0.07	**0.0116**	0.9872	5 (36)	8 (62)
CC body	1.75 ± 0.13	1.76 ± 0.12	1.61 ± 0.09	1.65 ± 0.13	**0.0037**	0.8271	6 (43)	8 (62)
CST	1.46 ± 0.05	1.48 ± 0.05	1.42 ± 0.04	1.42 ± 0.05	**0.0278**	0.4686	8 (57)	4 (31)
Radial diffusivity								
WM	0.76 ± 0.06	0.76 ± 0.06	0.75 ± 0.03	0.77 ± 0.04	0.0861	**0.0422**	4 (29)	11 (85)
CC splenium	0.74 ± 0.10	0.73 ± 0.10	0.77 ± 0.12	0.97 ± 0.20	0.8077	**0.0013**	**4 (29)**	**13 (100)**
CC genu	0.68 ± 0.06	0.67 ± 0.05	0.65 ± 0.04	0.70 ± 0.06	0.1495	**0.0441**	4 (29)	12 (92)
CC body	0.87 ± 0.14	0.85 ± 0.11	0.78 ± 0.09	0.85 ± 0.11	**0.0286**	**0.0288**	6 (43)	12 (92)
CST	0.66 ± 0.07	0.65 ± 0.07	0.63 ± 0.04	0.64 ± 0.04	**0.0271**	0.0671	5 (36)	8 (62)
Mean diffusivity								
WM	0.90 ± 0.05	0.89 ± 0.05	0.88 ± 0.03	0.89 ± 0.04	**0.0256**	0.1268	5 (36)	11 (85)
CC splenium	1.01 ± 0.10	1.01 ± 0.10	0.99 ± 0.09	1.17 ± 0.18	0.3410	**0.0013**	**3 (21)**	**13 (100)**
CC genu	0.92 ± 0.06	0.92 ± 0.04	0.88 ± 0.03	0.92 ± 0.06	**0.0226**	0.0938	4 (29)	11 (85)
CC body	1.11 ± 0.13	1.09 ± 0.10	1.00 ± 0.08	1.06 ± 0.10	**0.0120**	0.0945	5 (36)	11 (85)
CST	0.85 ± 0.05	0.85 ± 0.05	0.83 ± 0.03	0.83 ± 0.03	**0.0162**	0.1969	6 (43)	7 (54)

Abbreviations: ANCOVA = analysis of covariance; C-ALD = cerebral adrenoleukodystrophy; CC = corpus callosum; CST = corticospinal tract; DTI = diffusion tensor imaging; p_{BH} = Benjamini-Hochberg adjusted *p*-values; ROI = region of interest; WM = white matter.
Axial, radial, and mean diffusivity units are $\times 10^{-9}$ m^2/s. Fractional anisotropy, axial diffusivity, radial diffusivity, and mean diffusivity are reported for baseline and follow-up time points in the cerebral white matter, subdivisions of the corpus callosum, and the corticospinal tract. Results of group comparisons of baseline DTI metrics and slopes with ANCOVA are shown with adjusted *p*-values (values in bold show $p_{BH} < 0.05$). The frequency of patients in each group showing positive longitudinal change (frequency of slope >0) in each metric over the one year period is presented in the far-right 2 columns. Values in bold indicate slope measures with high sensitivity (SE) and specificity (SP) for the group determination, with the threshold set at SE + SP >170%. SE and SP can be derived from the positive slope frequency as follows: For FA, SE = 100% − mild lesion frequency and SP = no lesion frequency. For axial diffusivity, radial diffusivity, and mean diffusivity, SE = mild lesion frequency and SP = 100% − no lesion frequency.

The longitudinal results for AD, RD, and MD are shown in eFigures 5–7. MD and RD provided high discriminability for post-HCT changes among those with early-stage posterior C-ALD lesions (Table 2; eFigures 6 and 7). In the CC splenium, MD and RD slopes were $0.163 \pm 0.109 \times 10^{-9}$ $m^2/s{\cdot}y$ and $0.183 \pm 0.122 \times 10^{-9}$ $m^2/s{\cdot}y$ in mild posterior C-ALD and $-0.006 \pm 0.035 \times 10^{-9}$ $m^2/s{\cdot}y$ and $-0.009 \pm 0.029 \times 10^{-9}$ $m^2/s{\cdot}y$ in NL-ALD, respectively.

For all severity levels, eTable 1 shows baseline, follow-up, and slope imaging measurements, including uncorrected statistical comparisons.

Associations of MRI Metrics With Clinical Neurocognitive Outcomes

Associations between pre-HCT MRI metrics (Loes score and DTI metrics) and neurocognitive functions at 1-year after HCT

Figure 4 Longitudinal Change in FA in 5 ROIs Among Boys With ALD With and Without Demyelinating Lesions

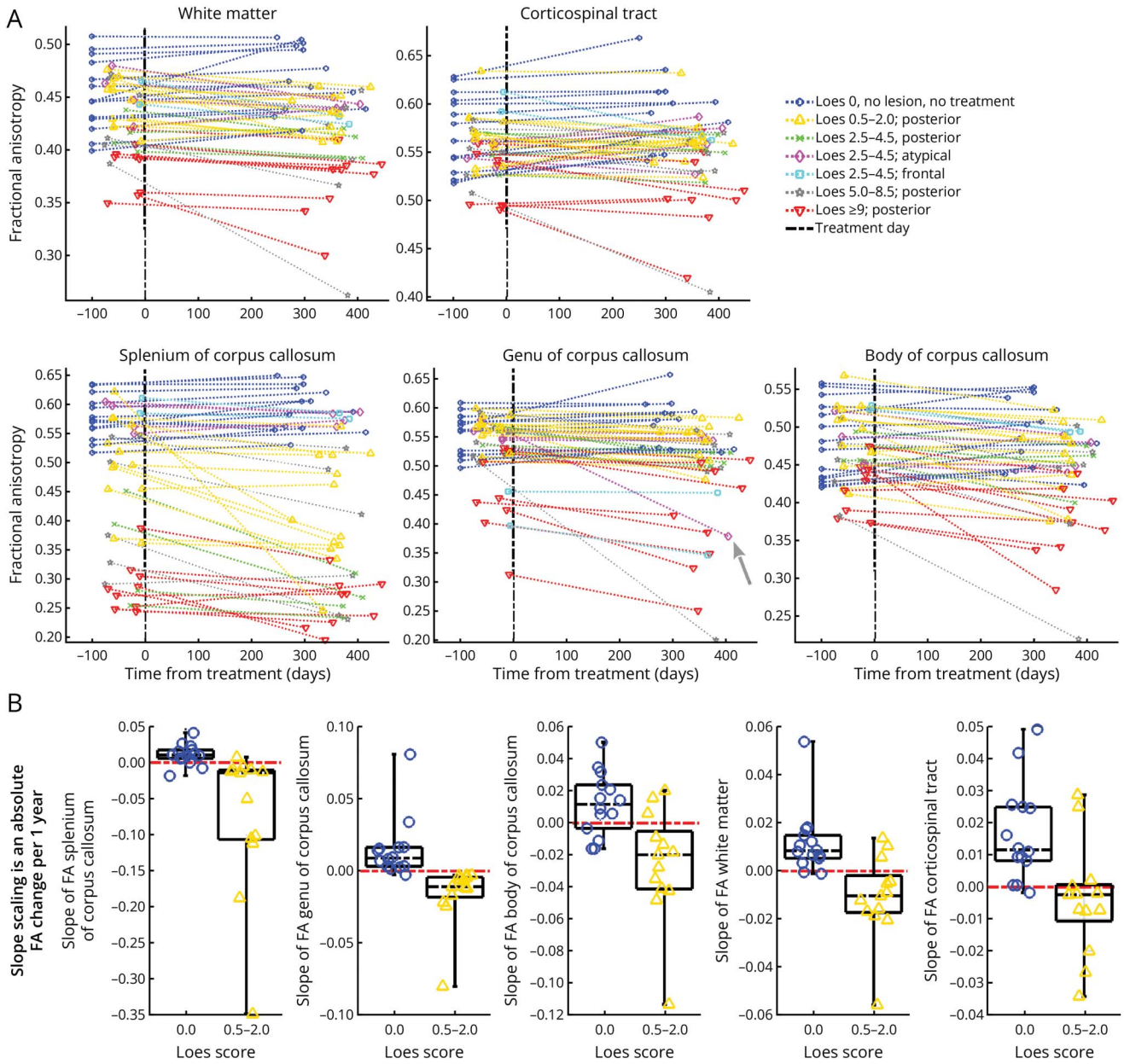

(A) Visualization of longitudinal change in FA metrics over a 1-year period based on the presence and severity of lesions assessed by the Loes score. For patients without lesions (dark blue) and those with frontal (cyan) and atypical (magenta) lesions, FA values in the CC splenium were generally similar at baseline and showed stable or positive slope trajectories. By contrast, lower baseline values and declines over time were frequently seen in patients with C-ALD with posterior lesions. In the genu, FA estimates were lower for patients with frontal lesions (cyan) and those with severe C-ALD (red). The gray arrow on the plot of genu FA values points to a patient with an atypical disease pattern who developed frontal demyelination between scans. The graph for the corticospinal tract ROI shows positive slopes for most patients with NL-ALD and negative (declining) slopes for most patients with C-ALD. The cerebral WM and CC body show results similar to the CC splenium with a weaker group separation. (B) Comparison of FA slope across ROIs in boys without cerebral lesions (dark blue) and those with mild posterior cerebral lesions (yellow). The red dashed line depicts a slope equal to 0. The time interval for the reported slope values was measured in years. ALD = adrenoleukodystrophy; C-ALD = cerebral adrenoleukodystrophy; CC = corpus callosum; DTI = diffusion tensor imaging; FA = fractional anisotropy; NL-ALD = adrenoleukodystrophy with no lesion; ROI = region of interest; WM = white matter.

are reported in Figure 5. Moderate to large effect sizes (0.5–0.8) were seen in correlations between pre-HCT Loes score and 4 post-HCT neuropsychological measures (i.e., visual reasoning, processing speed, fine motor dexterity, and visual-motor integration), with higher MRI severity associated with lower post-HCT neurocognitive test performance. Both cerebral WM and CC splenium DTI metrics (FA, MD, and RD) showed correlations of similar magnitude with these same neurocognitive outcomes. Better WM integrity metrics (i.e., higher FA or lower RD and MD) at the time of HCT were associated with better neurocognitive test results. Correlations were less robust between pre-HCT Loes/DTI metrics and post-HCT verbal reasoning and working memory. However, FA, RD, and MD in the cerebral WM and CC splenium were moderately associated

Figure 5 Correlation of Pre-HCT Loes Score and DTI Variables With Neurocognitive Measures 1 Year After HCT in 38 Boys With C-ALD

	Verbal reasoning (n = 32)		Visual reasoning (n = 34)		Working memory (n = 30)		Processing speed (n = 34)		Fine motor dexterity (n = 34)		Visual–motor integration (n = 34)	
Pre–HCT measure	R	99% CI	R	99% CI	R	99% CI	R	99% CI	R	99% CI	R	99% CI
Loes score	−0.19	(−0.59, 0.28)	−0.61	(−0.82, −0.24)	−0.31	(−0.67, 0.17)	−0.65	(−0.85, −0.30)	−0.48	(−0.75, −0.06)	−0.75	(−0.89, −0.48)
FA white matter	0.28	(−0.19, 0.64)	0.63	(0.27, 0.84)	0.51	(0.06, 0.78)	0.64	(0.28, 0.84)	0.58	(0.20, 0.81)	0.71	(0.40, 0.87)
FA splenium	0.08	(−0.38, 0.50)	0.52	(0.11, 0.78)	0.38	(−0.09, 0.72)	0.56	(0.17, 0.80)	0.45	(0.02, 0.74)	0.63	(0.27, 0.83)
FA genu	0.23	(−0.23, 0.62)	0.43	(0.00, 0.73)	0.35	(−0.13, 0.70)	0.58	(0.19, 0.81)	0.41	(−0.03, 0.71)	0.56	(0.17, 0.80)
FA body	0.23	(−0.24, 0.61)	0.40	(−0.04, 0.71)	0.35	(−0.13, 0.70)	0.31	(−0.14, 0.66)	0.22	(−0.23, 0.60)	0.43	(0.00, 0.73)
FA CST	0.22	(−0.25, 0.61)	0.45	(0.03, 0.74)	0.36	(−0.12, 0.70)	0.43	(0.00, 0.73)	0.38	(−0.07, 0.70)	0.58	(0.20, 0.81)
AD white matter	−0.14	(−0.55, 0.33)	−0.36	(−0.69, 0.08)	−0.16	(−0.58, 0.32)	−0.21	(−0.59, 0.25)	−0.36	(−0.69, 0.08)	−0.37	(−0.69, 0.07)
AD splenium	−0.27	(−0.64, 0.20)	−0.52	(−0.78, −0.12)	−0.37	(−0.71, 0.11)	−0.52	(−0.78, −0.11)	−0.51	(−0.77, −0.10)	−0.62	(−0.83, −0.25)
AD genu	−0.23	(−0.61, 0.24)	−0.07	(−0.49, 0.38)	−0.06	(−0.50, 0.41)	−0.03	(−0.45, 0.41)	−0.17	(−0.56, 0.29)	−0.13	(−0.53, 0.32)
AD body	−0.23	(−0.61, 0.24)	−0.30	(−0.65, 0.15)	−0.21	(−0.61, 0.27)	−0.21	(−0.59, 0.25)	−0.31	(−0.66, 0.14)	−0.35	(−0.68, 0.10)
AD CST	0.22	(−0.25, 0.61)	0.17	(−0.28, 0.56)	0.25	(−0.23, 0.64)	0.19	(−0.27, 0.57)	0.17	(−0.29, 0.56)	0.29	(−0.16, 0.64)
RD white matter	−0.25	(−0.62, 0.22)	−0.65	(−0.85, −0.31)	−0.54	(−0.80, −0.11)	−0.63	(−0.83, −0.27)	−0.62	(−0.83, −0.25)	−0.73	(−0.88, −0.43)
RD splenium	−0.11	(−0.53, 0.36)	−0.58	(−0.81, −0.19)	−0.46	(−0.76, −0.01)	−0.63	(−0.83, −0.27)	−0.50	(−0.77, −0.09)	−0.72	(−0.88, −0.41)
RD genu	−0.30	(−0.66, 0.17)	−0.45	(−0.74, −0.02)	−0.41	(−0.73, 0.06)	−0.60	(−0.82, −0.23)	−0.46	(−0.75, −0.04)	−0.56	(−0.80, −0.17)
RD body	−0.27	(−0.64, 0.20)	−0.43	(−0.73, 0.00)	−0.32	(−0.68, 0.16)	−0.35	(−0.68, 0.10)	−0.31	(−0.65, 0.14)	−0.47	(−0.75, −0.05)
RD CST	−0.06	(−0.49, 0.40)	−0.47	(−0.75, −0.04)	−0.28	(−0.66, 0.20)	−0.38	(−0.70, 0.06)	−0.34	(−0.67, 0.11)	−0.51	(−0.77, −0.09)
MD white matter	−0.27	(−0.64, 0.20)	−0.64	(−0.84, −0.29)	−0.53	(−0.79, −0.09)	−0.56	(−0.80, −0.17)	−0.59	(−0.81, −0.21)	−0.73	(−0.88, −0.43)
MD splenium	−0.15	(−0.56, 0.31)	−0.61	(−0.83, −0.24)	−0.51	(−0.78, −0.06)	−0.64	(−0.84, −0.29)	−0.56	(−0.80, −0.16)	−0.74	(−0.89, −0.45)
MD genu	−0.27	(−0.64, 0.20)	−0.37	(−0.69, 0.08)	−0.33	(−0.68, 0.16)	−0.51	(−0.77, −0.10)	−0.40	(−0.71, 0.03)	−0.52	(−0.78, −0.11)
MD body	−0.26	(−0.63, 0.21)	−0.43	(−0.72, 0.01)	−0.30	(−0.67, 0.18)	−0.30	(−0.65, 0.15)	−0.32	(−0.66, 0.13)	−0.46	(−0.74, −0.03)
MD CST	−0.04	(−0.48, 0.41)	−0.39	(−0.70, 0.06)	−0.21	(−0.61, 0.27)	−0.25	(−0.62, 0.20)	−0.28	(−0.64, 0.17)	−0.40	(−0.71, 0.04)

Spearman correlation coefficient (R) and corresponding 99% confidence interval (CI) are calculated for each row-column pair

Color key: −1 ≤ R ≤ −0.75 or 0.75 ≤ R ≤ 1.0; −0.75 < R ≤ −0.50 or 0.50 ≤ R <0.75; −0.50 < R ≤ −0.25 or 0.25 ≤ R < 0.50; −0.25 < R < 0.25

AD = axial diffusivity; CST = corticospinal tract; DTI = diffusion tensor imaging; FA = fractional anisotropy; HCT = hematopoietic cell transplant; MD = mean diffusivity; RD = radial diffusivity.

with working memory. Besides visual-motor integration, the pre-HCT DTI metrics, mainly from the cerebral white matter (FA, RD, AD) and CC splenium (MD, AD), revealed comparable or even higher associations with 1-year post-HCT neurocognitive functions than the pre-HCT Loes score.

Examination of longitudinal change in Loes score and DTI metrics relative to *changes* in neurocognitive scores over 1 year revealed a similar pattern of findings (eFigure 8), with more modest associations. Increases in Loes score, MD, and RD and decreases in FA were associated with declines in neurocognitive abilities. For 2 measures (visual reasoning and processing speed), Loes score changes showed the strongest correlations with neurocognitive changes. For the remaining 4 measures (verbal reasoning, working memory, fine motor dexterity, and visual-motor integration), DTI changes showed similar or higher correlations with neurocognitive changes than Loes scores. For total WM, changes in RD and MD were modestly correlated with changes across all 6 neurocognitive domains.

Discussion

This study demonstrates the sensitivity of DTI metrics to the presence of early C-ALD lesions. These metrics quantify disease severity and associate with neurocognitive effects after treatment of C-ALD.

Our findings demonstrate that DTI provides a sensitive, objective method to quantify early C-ALD lesions. The sensitivity of DTI increases within ROIs that correspond to the location of the earliest lesions. In ~80% of individuals with C-ALD, lesions are first observed in the densely packed fibers of the CC splenium and progress into periventricular parietal-occipital WM (posterior pattern).[18] In the remaining individuals, lesions emerge in the CC genu or pyramidal tracts (frontal and atypical pattern, respectively). In this study, when comparing a subgroup of patients with the mildest posterior lesions (Loes = 1–2) with patients without lesions, group differences were apparent across several DTI parameters. FA in the CC splenium was lower in most boys with mild posterior lesions as compared with those without lesions. Lower AD was also observed across several ROIs, including ROIs where lesions were not seen on radiologic review (e.g., CC genu and CST). Group differences remained after controlling for age and when examining only voxels without visible lesions. This finding builds on prior studies describing differences between individuals with C-ALD and controls in DTI metrics within normal-appearing WM ROIs.[14,15] Thus, these results support our first 2 working hypotheses.

The observation that DTI differences can be detected in normal-appearing white matter suggests the promise of DTI as a potential tool to assist with early diagnosis of an emerging C-ALD lesion. Further exploration of DTI within the research setting could assess the potential benefit of using DTI alongside conventional MRI to, for example, detect changes that might prompt closer scrutiny or more frequent surveillance scans. Prospective studies using a cohort of boys developing early MRI changes during the monitoring period would be especially valuable to evaluate whether subtle changes in the slope of DTI metrics identify the onset of C-ALD. Nevertheless, some caution is needed in considering an adaptation of DTI as a tool for clinical practice. Although clear differences between NL-ALD and mild C-ALD groups across DTI metrics were evident in our study at the group level, some overlap in distributions for each DTI metric was apparent (Figure 4). This finding suggests that the DTI results at a single time point would not have been sufficient to inform treatment-related decision making at the individual patient level (i.e., independent from the radiologic review). Given the substantial risks of the treatments presently available for C-ALD, current clinical management guidelines recommend confirmation of an active and progressive (usually contrast-enhancing) lesion before proceeding with intervention.[35,36]

Cross-sectional analysis allowed comparison of DTI metrics of patients with C-ALD experiencing different stages of disease severity. Notably, DTI metrics vary in their correspondence to different properties of WM microstructure. Specifically, RD and AD quantify the ease of water diffusion across or along axons and are believed to reflect the integrity of myelin and axons, respectively.[33,37] FA has been reported to be an indicator of axonal count and density as well as myelin content.[38] In our data set, higher disease severity, as measured by the Loes score, was associated with higher FA and lower RD. AD showed a somewhat different pattern. The results suggest that diffusivity along axons may initially decrease during early illness, perhaps because of axonal damage. Later in the disease, AD may increase as lesions become more severe, reflecting loss of axons. This finding aligns with research regarding the pathophysiology of ALD lesions. Three histopathologic zones with a spatiotemporal sequence can be observed in C-ALD lesions.[39,40] An outermost zone at the peripheral edge (prelesional area) shows acute axonal damage associated with early microglia loss.[41] Moving inward, a second zone is characterized by demyelinated axons, permanent axon loss, and inflammation. The center of the lesion (inner core) is characterized by near-complete loss of axons and myelin sheaths as well as astrocytic scarring. Previous studies showed an association between DTI metrics and these histopathologic zones, with lower FA at the lesion core than the lesion periphery.[16,39,42] In postmortem analyses, lower FA has also associated with histopathologic metrics including lower myelin and axon density and more severe astrogliosis.[39]

Our analysis found that nearly all individuals in the NL-ALD group showed stable or increasing longitudinal FA values across the ROIs examined, supporting our third working hypothesis. This finding aligns with studies of healthy 4- to-11-year-old children, which have reported a relatively small annual percentage change in FA values in the CC splenium and genu relative to other fiber tracts (e.g., association fibers).[43] The stability of FA values in the CC splenium and genu during this period may reflect earlier maturation of CC tracts relative to other fiber tracts.[44,45] These findings lead to the hypothesis that changes in slope direction of DTI metrics will provide valuable information about the potential for the emergence of a lesion even before observable WM changes. Further prospective research is needed to study the value of DTI, ideally in combination with other biomarkers, in disease surveillance.

Given that DTI metrics can be affected by chemotherapy agents[46] and MRI progression may not stabilize until 6–18 months after HCT,[9] we expected that DTI metrics would show declining white matter integrity over time among some patients with C-ALD. A comparison of longitudinal change (slopes) in DTI metrics between the NL-ALD group and the mild C-ALD group found group differences across all ROIs. For any individual with C-ALD, the direction of longitudinal change in DTI metrics in the post-HCT period could reflect the effects of chemotherapy/HCT, further disease progression, or a combination of both factors. In future studies, continued monitoring of DTI metrics further out from HCT could facilitate a better understanding of the expected time course of post-HCT stability and change at each risk level. This understanding could increase the utility of DTI as a potential quantitative marker of treatment response in clinical trials, for example, to assess the relative effectiveness of a new therapy.

Several prior studies have shown that pre-HCT Loes MRI severity scores correlate with neurocognitive outcomes.[10,22,47,48] Our data extend these observations, showing a robust relationship between pre-HCT DTI metrics and post-HCT neurocognitive scores. A previous longitudinal study involving a small cohort (n = 8) of patients with C-ALD found limited evidence for an association of DTI metrics with neurocognitive outcomes.[13] Only 1 pre-HCT metric (callosal body FA) was associated with clinical outcomes at 1-year after HCT. The present study using a substantially larger data set (n = 38) detected correlations between pre-HCT DTI metrics and post-HCT neurocognitive scores across multiple domains, supporting our fourth working hypothesis. Aligned with previous studies, associations between brain-based and neurocognitive metrics were strongest for neurocognitive tests involving visual processing, performance speed, and fine motor dexterity.[49] These findings further differentiate the most sensitive clinical indicators of disease burden among patients identified early in the course of the disease.

Pre-HCT DTI metrics showed comparable or even stronger associations to post-HCT neurocognitive outcomes relative to Loes scores. Furthermore, longitudinal changes in Loes scores and DTI metrics were both correlated with changes in neurocognitive functioning over the course of the 1-year post-

HCT period, suggesting that brain changes and functional changes were dynamically related. The strength of the associations depended to some extent on which neurocognitive domain was being assessed. Whereas DTI metrics (e.g., MD in WM) generally showed stronger associations with verbal reasoning and working memory outcomes, Loes scores generally showed stronger associations with visual reasoning and processing speed (Figure 5).

Given that Loes scores and DTI metrics had somewhat comparable associations with outcomes, their relative advantages in clinical and research settings may depend on practical considerations. Loes scores are based on visual inspection of anatomical MRI scans by a neuroradiologist, which can vary based on individual raters' impression and extent of experience with this disease-specific scoring system.[50] By contrast, the DTI protocol used in this study allowed for fully automated, objective results. Although some experience with diffusion MRI is necessary, metrics can be obtained using our acquisition protocol and DTI model even with older (e.g., 1.5T) clinical scanners, making this methodology widely applicable across clinical centers.

This study was performed in a 3T MRI scanner with 12-direction DTI acquisition. Although this protocol has a higher in-plane resolution than previous studies conducted on 1.5–3T scanners with 6 different directions,[13,14] the protocol could be enhanced with further optimization. Future diffusion MRI protocols would benefit from thinner slice thickness, an isotropic voxel size, multishell acquisition with higher b value(s), and high angular diffusion resolution imaging (i.e., more diffusion directions). Improved diffusion acquisition protocols provide reproducible tractography, and thus, reproducible assessment of tract-specific morphology and microstructure as well as the use of biologically inspired diffusion modeling. The linear approximation of longitudinal DTI changes may not be accurate; however, nonlinear longitudinal development cannot be assessed from only 2 temporal measurements. Adding more time points may uncover complex trajectories in diffusion metric changes over time. Owing to a wide variety of HCT protocols in our patients with C-ALD, it was not feasible to account for heterogeneity in treatment parameters (e.g., allogeneic vs autologous HCT; chemotherapy regimens; graft source) contributing to the variation in DTI metrics and neurocognitive outcomes at the follow-up time point. The small sample size and differences in the eligibility of patients for specific treatment protocols prevented subgroup comparisons based on specific treatment types. Future research involving suitably matched cohorts should assess for potential differences in radiologic findings of patients receiving different forms of cell therapy. In addition, the lack of a healthy control group precluded a comparative assessment of white matter integrity in the NL-ALD group and typically developing children. Finally, a multimodal protocol, including optimized diffusion MRI, other myelin-specific MRI techniques, and MR spectroscopy, may unravel the underpinnings of ALD pathophysiology and provide noninvasive markers crucial in disease monitoring.

Quantitative neuroimaging techniques such as diffusion MRI may serve as useful tools for assessing disease onset, progression, and severity for C-ALD. Of the DTI metrics used in this study, FA and AD in the CC splenium demonstrated particular sensitivity for distinguishing early posterior disease. Furthermore, these metrics generally remained stable in longitudinal analysis of individuals with ALD who did not have cerebral lesions. Diffusion imaging metrics may also prove to be successful predictors of clinical outcomes. The correlations between DTI metrics and neurocognitive outcomes found in this study were similar in magnitude to those previously demonstrated using the Loes score. Further studies using optimized diffusion MRI protocols (alone and in combination with other biomarkers) are needed to identify the most robust indicators of disease onset and disease progression. These findings suggest opportunities to improve surveillance protocols as well as quantify brain changes in response to treatment.

Acknowledgment

The authors are grateful to Christophe Lenglet for his consultation and guidance on the concepts of DTI analysis. The authors also thank Evelyn Elizondo, Dante Rogers, and Carol Nguyen for data curation and management and Ixchel Salter for assistance with lesion outlining.

Study Funding

This research was supported by the National Institutes of Health (K23NS123258 and UL1TR002494) and the University of Minnesota Foundation. The content is solely the responsibility of the authors and does not necessarily represent the official views of the National Institutes of Health. A subset of individuals reported in this study participated in clinical trials sponsored by bluebird bio; this sponsor was not involved in the acquisition or analysis of the data.

Disclosure

E.I. Pierpont has consulted for bluebird bio. D. Loes has consulted for bluebird bio, Minoryx, and Swanbio. All other authors report no relevant disclosures. Go to Neurology.org/N for full disclosures.

Publication History

Received by *Neurology* March 11, 2024. Accepted in final form June 18, 2024. Submitted and externally peer reviewed. The handling editor was Associate Editor Courtney Wusthoff, MD, MS.

Appendix Authors

Name	Location	Contribution
Elizabeth I. Pierpont, PhD	Department of Pediatrics, University of Minnesota Medical School, Minneapolis	Drafting/revision of the manuscript for content, including medical writing for content; major role in the acquisition of data; study concept or design; analysis or interpretation of data

Continued

Appendix *(continued)*

Name	Location	Contribution
René Labounek, PhD	Department of Pediatrics, University of Minnesota Medical School, Minneapolis	Drafting/revision of the manuscript for content, including medical writing for content; study concept or design; analysis or interpretation of data
Ashish Gupta, MD, MPH	Department of Pediatrics, University of Minnesota Medical School, Minneapolis	Drafting/revision of the manuscript for content, including medical writing for content; major role in the acquisition of data
Troy Lund, MD, PhD	Department of Pediatrics, University of Minnesota Medical School, Minneapolis	Drafting/revision of the manuscript for content, including medical writing for content; major role in the acquisition of data
Paul J. Orchard, MD	Department of Pediatrics, University of Minnesota Medical School, Minneapolis	Drafting/revision of the manuscript for content, including medical writing for content; major role in the acquisition of data
William B. Dobyns, MD	Department of Pediatrics, University of Minnesota Medical School, Minneapolis	Drafting/revision of the manuscript for content, including medical writing for content; analysis or interpretation of data
Monica Bondy, BS	Department of Pediatrics, University of Minnesota Medical School, Minneapolis	Drafting/revision of the manuscript for content, including medical writing for content; major role in the acquisition of data; analysis or interpretation of data
Amy Paulson, BS	Department of Pediatrics, University of Minnesota Medical School, Minneapolis	Analysis or interpretation of data
Andrew Metz, MD	Department of Neurology, University of Minnesota Medical School, Minneapolis	Drafting/revision of the manuscript for content, including medical writing for content; analysis or interpretation of data
Ryan Shanley, MS	Biostatistical Design and Analysis Center, Clinical and Translational Science Institute, University of Minnesota, Minneapolis	Drafting/revision of the manuscript for content, including medical writing for content; analysis or interpretation of data
Jeffrey R. Wozniak, PhD	Department of Psychiatry & Behavioral Sciences, University of Minnesota Medical School, Minneapolis	Drafting/revision of the manuscript for content, including medical writing for content; analysis or interpretation of data
Bryon A. Mueller, PhD	Department of Psychiatry & Behavioral Sciences, University of Minnesota Medical School, Minneapolis	Drafting/revision of the manuscript for content, including medical writing for content; major role in the acquisition of data; analysis or interpretation of data
Daniel Loes, MD	Independent Neuroradiologist-Consultant, Minneapolis, MN	Analysis or interpretation of data
David Nascene, MD	Department of Radiology, University of Minnesota Medical School, Minneapolis	Drafting/revision of the manuscript for content, including medical writing for content; major role in the acquisition of data; analysis or interpretation of data
Igor Nestrasil, MD, PhD	Department of Pediatrics, University of Minnesota Medical School, Minneapolis	Drafting/revision of the manuscript for content, including medical writing for content; major role in the acquisition of data; study concept or design; analysis or interpretation of data

References

1. Engelen M, Kemp S, Poll-The BT. X-linked adrenoleukodystrophy: pathogenesis and treatment. *Curr Neurol Neurosci Rep*. 2014;14(10):486. doi:10.1007/s11910-014-0486-0
2. Mallack EJ, Van Haren KP, Torrey A, et al. Presymptomatic lesion in childhood cerebral adrenoleukodystrophy: timing and treatment. *Neurology*. 2022;99(5):e512-e520. doi:10.1212/WNL.0000000000200571
3. Turk BR, Theda C, Fatemi A, Moser AB. X-linked adrenoleukodystrophy: pathology, pathophysiology, diagnostic testing, newborn screening and therapies. *Int J Dev Neurosci*. 2020;80(1):52-72. doi:10.1002/jdn.10003
4. Eichler F, Duncan C, Musolino PL, et al. Hematopoietic stem-cell gene therapy for cerebral adrenoleukodystrophy. *N Engl J Med*. 2017;377(17):1630-1638. doi:10.1056/NEJMoa1700554
5. Peters C, Charnas LR, Tan Y, et al. Cerebral X-linked adrenoleukodystrophy: the international hematopoietic cell transplantation experience from 1982 to 1999. *Blood*. 2004;104(3):881-888. doi:10.1182/blood-2003-10-3402
6. Gupta AO, Raymond G, Pierpont EI, et al. Treatment of cerebral adrenoleukodystrophy: allogeneic transplantation and lentiviral gene therapy. *Expert Opin Biol Ther*. 2022;22(9):1151-1162. doi:10.1080/14712598.2022.2124857
7. Pierpont EI, Nascene DR, Shanley R, et al. Neurocognitive benchmarks following transplant for emerging cerebral adrenoleukodystrophy. *Neurology*. 2020;95(5):e591-e600. doi:10.1212/WNL.0000000000009929
8. Loes DJ, Hite S, Moser H, et al. Adrenoleukodystrophy: a scoring method for brain MR observations. *AJNR Am J Neuroradiol*. 1994;15(9):1761-1766.
9. Raymond GV, Aubourg P, Paker A, et al. Survival and functional outcomes in boys with cerebral adrenoleukodystrophy with and without hematopoietic stem cell transplantation. *Biol Blood Marrow Transplant*. 2019;25(3):538-548. doi:10.1016/j.bbmt.2018.09.036
10. Pierpont EI, Eisengart JB, Shanley R, et al. Neurocognitive trajectory of boys who received a hematopoietic stem cell transplant at an early stage of childhood cerebral adrenoleukodystrophy. *JAMA Neurol*. 2017;74(6):710-717. doi:10.1001/jamaneurol.2017.0013
11. Moser AB, Seeger E, Raymond GV. Newborn screening for X-linked adrenoleukodystrophy: past, present, and future. *Int J Neonatal Screen*. 2022;8(1):16. doi:10.3390/ijns8010016
12. Swenson A, Nascene D. Early brain findings in cerebral adrenoleukodystrophy: are we missing subtle disease? Abstract Presented at: American Society of Neuroradiology 57th Annual Meeting; Boston, MA; 2019.
13. van de Stadt SIW, Huffnagel IC, Turk BR, van der Knaap MS, Engelen M. Imaging in X-linked adrenoleukodystrophy. *Neuropediatrics*. 2021;52(4):252-260. doi:10.1055/s-0041-1730937
14. Schneider JF, Il'yasov KA, Boltshauser E, Hennig J, Martin E. Diffusion tensor imaging in cases of adrenoleukodystrophy: preliminary experience as a marker for early demyelination? *AJNR Am J Neuroradiol*. 2003;24(5):819-824.
15. McKinney AM, Nascene D, Miller WP, et al. Childhood cerebral X-linked adrenoleukodystrophy: diffusion tensor imaging measurements for prediction of clinical outcome after hematopoietic stem cell transplantation. *AJNR Am J Neuroradiol*. 2013;34(3):641-649. doi:10.3174/ajnr.A3232
16. Ito R, Melhem ER, Mori S, Eichler FS, Raymond GV, Moser HW. Diffusion tensor brain MR imaging in X-linked cerebral adrenoleukodystrophy. *Neurology*. 2001;56(4):544-547. doi:10.1212/wnl.56.4.544
17. Huffnagel IC, van Ballegoij WJC, Vos J, Kemp S, Caan MWA, Engelen M. Longitudinal diffusion MRI as surrogate outcome measure for myelopathy in adrenoleukodystrophy. *Neurology*. 2019;93(23):e2133-e2143. doi:10.1212/WNL.0000000000008572

18. Loes DJ, Fatemi A, Melhem ER, et al. Analysis of MRI patterns aids prediction of progression in X-linked adrenoleukodystrophy. *Neurology*. 2003;61(3):369-374. doi:10.1212/01.wnl.0000079050.91337.83
19. Oouchi H, Yamada K, Sakai K, et al. Diffusion anisotropy measurement of brain white matter is affected by voxel size: underestimation occurs in areas with crossing fibers. *AJNR Am J Neuroradiol*. 2007;28(6):1102-1106. doi:10.3174/ajnr.A0488
20. Mukherjee P, Chung SW, Berman JI, Hess CP, Henry RG. Diffusion tensor MR imaging and fiber tractography: technical considerations. *AJNR Am J Neuroradiol*. 2008;29(5):843-852. doi:10.3174/ajnr.A1052
21. Gupta AO, Nascene DR, Shanley R, et al. Differential outcomes for frontal versus posterior demyelination in childhood cerebral adrenoleukodystrophy. *J Inherit Metab Dis*. 2021;44(6):1434-1440. doi:10.1002/jimd.12435
22. Kühl JS, Kupper J, Baque H, et al. Potential risks to stable long-term outcome of allogeneic hematopoietic stem cell transplantation for children with cerebral X-linked adrenoleukodystrophy. *JAMA Netw Open*. 2018;1(3):e180769. doi:10.1001/jamanetworkopen.2018.0769
23. Yushkevich PA, Piven J, Hazlett HC, et al. User-guided 3D active contour segmentation of anatomical structures: significantly improved efficiency and reliability. *Neuroimage*. 2006;31(3):1116-1128. doi:10.1016/j.neuroimage.2006.01.015
24. Jenkinson M, Beckmann CF, Behrens TE, Woolrich MW, Smith SM. FSL. *Neuroimage*. 2012;62(2):782-790. doi:10.1016/j.neuroimage.2011.09.015
25. Smith SM. Fast robust automated brain extraction. *Hum Brain Mapp*. 2002;17(3):143-155. doi:10.1002/hbm.10062
26. Mori S, Wakana S, Zijl PCM, Nagae-Poetscher LM. *MRI Atlas of Human White Matter*. Elsevier; 2005.
27. Wakana S, Caprihan A, Panzenboeck MM, et al. Reproducibility of quantitative tractography methods applied to cerebral white matter. *Neuroimage*. 2007;36(3):630-644. doi:10.1016/j.neuroimage.2007.02.049
28. Hua K, Zhang J, Wakana S, et al. Tract probability maps in stereotaxic spaces: analyses of white matter anatomy and tract-specific quantification. *Neuroimage*. 2008;39(1):336-347. doi:10.1016/j.neuroimage.2007.07.053
29. Jenkinson M, Smith S. A global optimisation method for robust affine registration of brain images. *Med Image Anal*. 2001;5(2):143-156. doi:10.1016/s1361-8415(01)00036-6
30. Jenkinson M, Bannister P, Brady M, Smith S. Improved optimization for the robust and accurate linear registration and motion correction of brain images. *Neuroimage*. 2002;17(2):825-841. doi:10.1016/s1053-8119(02)91132-8
31. Andersson JLR, Jenkinson M, Smith S. Non-linear registration, aka spatial normalisation. FMRIB Technical Report TR07JA2. 2010.
32. Power MC, Su D, Wu A, et al. Association of white matter microstructural integrity with cognition and dementia. *Neurobiol Aging*. 2019;83:63-72. doi:10.1016/j.neurobiolaging.2019.08.021
33. Tamnes CK, Roalf DR, Goddings AL, Lebel C. Diffusion MRI of white matter microstructure development in childhood and adolescence: methods, challenges and progress. *Dev Cogn Neurosci*. 2018;33:161-175. doi:10.1016/j.dcn.2017.12.002
34. Lebel C, Deoni S. The development of brain white matter microstructure. *Neuroimage*. 2018;182:207-218. doi:10.1016/j.neuroimage.2017.12.097
35. Engelen M, van Ballegoij WJC, Mallack EJ, et al. International recommendations for the diagnosis and management of patients with adrenoleukodystrophy: a consensus-based approach. *Neurology*. 2022;99(21):940-951. doi:10.1212/WNL.0000000000201374
36. Mallack EJ, Turk BR, Yan H, et al. MRI surveillance of boys with X-linked adrenoleukodystrophy identified by newborn screening: meta-analysis and consensus guidelines. *J Inherit Metab Dis*. 2021;44(3):728-739. doi:10.1002/jimd.12356
37. Song SK, Sun SW, Ramsbottom MJ, Chang C, Russell J, Cross AH. Dysmyelination revealed through MRI as increased radial (but unchanged axial) diffusion of water. *Neuroimage*. 2002;17(3):1429-1436. doi:10.1006/nimg.2002.1267
38. Winston GP. The physical and biological basis of quantitative parameters derived from diffusion MRI. *Quant Imaging Med Surg*. 2012;2(4):254-265. doi:10.3978/j.issn.2223-4292.2012.12.05
39. van der Voorn JP, Pouwels PJ, Powers JM, et al. Correlating quantitative MR imaging with histopathology in X-linked adrenoleukodystrophy. *AJNR Am J Neuroradiol*. 2011;32(3):481-489. doi:10.3174/ajnr.A2327
40. Ferrer I, Aubourg P, Pujol A. General aspects and neuropathology of X-linked adrenoleukodystrophy. *Brain Pathol*. 2010;20(4):817-830. doi:10.1111/j.1750-3639.2010.00390.x
41. Bergner CG, Genc N, Hametner S, et al. Concurrent axon and myelin destruction differentiates X-linked adrenoleukodystrophy from multiple sclerosis. *Glia*. 2021;69(10):2362-2377. doi:10.1002/glia.24042
42. Eichler FS, Itoh R, Barker PB, et al. Proton MR spectroscopic and diffusion tensor brain MR imaging in X-linked adrenoleukodystrophy: initial experience. *Radiology*. 2002;225(1):245-252. doi:10.1148/radiol.2251011040
43. Krogsrud SK, Fjell AM, Tamnes CK, et al. Changes in white matter microstructure in the developing brain: a longitudinal diffusion tensor imaging study of children from 4 to 11 years of age. *Neuroimage*. 2016;124(pt A):473-486. doi:10.1016/j.neuroimage.2015.09.017
44. Rollins NK, Glasier P, Seo Y, Morriss MC, Chia J, Wang Z. Age-related variations in white matter anisotropy in school-age children. *Pediatr Radiol*. 2010;40(12):1918-1930. doi:10.1007/s00247-010-1744-1
45. Lebel C, Treit S, Beaulieu C. A review of diffusion MRI of typical white matter development from early childhood to young adulthood. *NMR Biomed*. 2019;32(4):e3778. doi:10.1002/nbm.3778
46. Deprez S, Billiet T, Sunaert S, Leemans A. Diffusion tensor MRI of chemotherapy-induced cognitive impairment in non-CNS cancer patients: a review. *Brain Imaging Behav*. 2013;7(4):409-435. doi:10.1007/s11682-012-9220-1
47. Pierpont EI, McCoy E, King KE, et al. Post-transplant adaptive function in childhood cerebral adrenoleukodystrophy. *Ann Clin Transl Neurol*. 2018;5(3):252-261. doi:10.1002/acn3.526
48. Miller WP, Rothman SM, Nascene D, et al. Outcomes after allogeneic hematopoietic cell transplantation for childhood cerebral adrenoleukodystrophy: the largest single-institution cohort report. *Blood*. 2011;118(7):1971-1978. doi:10.1182/blood-2011-01-329235
49. Pierpont EI, Isaia AR, McCoy E, Brown SJ, Gupta AO, Eisengart JB. Neurocognitive and mental health impact of adrenoleukodystrophy across the lifespan: insights for the era of newborn screening. *J Inher Metab Dis*. 2023;46(2):174-193. doi:10.1002/jimd.12581
50. Lin DDM, Nascene D, Eichler FS, et al. Variability of Loes scores and gadolinium enhancement status in MRI assessment of cerebral adrenoleukodystrophy following gene therapy or allogeneic hematopoietic stem cell transplantation. Abstract presented at the American Society of Neuroradiology; Virtual Meeting; 2021.